Published in final edited form as:
J Am Chem Soc. 2012 December 5; 134(48): 19839–19850. doi:10.1021/ja309082k.

Gas phase studies of substrates for the DNA mismatch repair enzyme MutY

Anna Zhachkina Michelson[‡], **Aleksandr Rozenberg**[‡], **Yuan Tian**[‡], **Xujeun Sun**[‡], **Julianne Davis**[‡], **Anthony W. Francis**[€], **Valerie O'Shea**[€], **Mohan Halasyam**[€], **Amelia H. Manlove**[X], **Sheila David**[X,€], and **Jeehiun K. Lee**[‡]

[‡]Department of Chemistry and Chemical Biology Rutgers, The State University of New Jersey, New Brunswick, NJ 08901

[€]Department of Chemistry, University of Utah, Salt Lake City, UT 84112

[X]Department of Chemistry, University of California, Davis, CA 95616

Abstract

The gas phase thermochemical properties (tautomeric energies, acidity, and proton affinity) have been measured and calculated for adenine and six adenine analogs that were designed to test features of the catalytic mechanism used by the adenine glycosylase MutY. The gas phase intrinsic properties are correlated to possible excision mechanisms and MutY excision rates to gain insight into the the MutY mechanism. The data support a mechanism involving protonation at N7 and hydrogen bonding to N3 of adenine. We also explored the acid-catalyzed (non-enzymatic) depurination of these substrates, which appears to follow a different mechanism than that employed by MutY, which we elucidate using calculations.

Introduction

Cellular DNA is inevitably damaged by both exogenous and endogenous agents, resulting in a variety of chemical modifications that are associated with mutagenesis, carcinogenesis and aging.[1-4] Oxidative damage is extremely prevalent, and one of the most common species formed by reactive oxygen species is 7,8-dihydro-8-oxo-guanine (OG).[5-7] During DNA replication, adenine (A) is usually inserted opposite OG to form a relatively stable OG:A mismatch.[8] Because undamaged guanine (G) prefers to pair with cytosine (C), not adenine, the oxidation, if not repaired, can result in permanent G:C →T:A transversion mutations.

In the face of the constant assault to DNA, organisms have developed elaborate DNA repair pathways. In *Escherichia coli*, oxidative damage is repaired by a “GO” repair pathway that utilizes three enzymes: MutT, Fpg, and MutY.[9-11] MutT hydrolyzes the OG deoxynucleoside triphosphate to yield the OG deoxynucleoside monophosphate and

Correspondence to: Sheila David; Jeehiun K. Lee.

SUPPORTING INFORMATION AVAILABLE

Cartesian coordinates for all calculated species, experimental details, acid-catalyzed depurination assays (Figure S1, S2) and full citations for references with greater than 16 authors are available. This material is available free of charge via the Internet at http://pubs.acs.org.

pyrophosphate, preventing its incorporation into replicating DNA.[12] Fpg (also called MutM) catalyzes removal of OG from OG:C base pairs, and an associated β and δ-lyase activity at the resultant abasic site leading to strand scission.[1,13] MutY is a somewhat unusual glycosylase enzyme; rather than targeting a damaged base, MutY catalyzes removal of adenine from OG:A mispairs in DNA (Figure 1).[1,12,13] MutY is remarkably specific such that 2'-deoxyadenosine residues within A:T pairs are not touched.

Because of the importance of damaged base repair to genome integrity, the mechanisms of repair enzymes are of great interest.[11] MutY crystal structures, in particular a 2009 *Bacillus stearothermophilus* structure with a fluorinated 2'-deoxyadenosine, show multiple hydrogen bonding contacts as well as hydrophobic interactions between substrate and enzyme.[14] Kinetic isotope effect studies imply an S_N1-type reaction where the nucleobase leaves (possibly protonated at N7) to yield an oxacarbenium ion which is then attacked by water.[14-16] Recent computational simulations support N7 protonation as well as an active site that organizes solvent to place water molecules into key catalytic positions.[17]

The examination of properties in the gas phase, which provides the "ultimate" nonpolar environment, reveals intrinsic reactivity that can be correlated to activity in other media, such as hydrophobic active sites.[18-24] In this paper, we calculate and measure the gas phase acidities and proton affinities of a series of adenine analogs (not heretofore studied in vacuo) and compare these results to the relative rates of MutY-catalyzed base excision of these analogs within the context of duplex DNA paired with OG. The acid-catalyzed non-enzymatic cleavage of these substrates is also explored.

Results

Adenine and the synthetically derived analogs studied herein are shown in Figure 2.[25-27] 7-Deazaadenine (Z), 3-deazaadenine (Z3) and 1-deazaadenine (Z1) are missing nitrogen at the N7, N3 and N1 positions, respectively (as compared to the parent adenine), and were designed to test the importance of the nitrogen at those positions.[26-28] Substrates Q, M and B (with atoms numbered as for adenine, to be consistent) are nonpolar isosteres of adenine.[25,27]

7-deazaadenine (Z, 1)

i. Calculations: Z tautomers, acidity, proton affinity—In our experience DFT methods generally yield accurate values for thermochemical properties of nucleobases, so we utilized B3LYP/6-31+G(d) to calculate the relative tautomeric stabilities, acidities (ΔH_{acid}), and proton affinities (PA) of 7-deazaadenine (Z, **1**).[18,22,23,29,30] (Throughout the paper, acidity and basicity are calculated only for those tautomers within 10 kcal mol^{-1} of the most stable tautomer). Z has eight possible tautomeric structures (Figure 3). The most stable tautomer (**1a**) is over 10 kcal mol^{-1} more stable than the next most stable species. We also calculated the acidity and basicity of the most stable tautomer. The most acidic site of **1a** is predicted to be the N9-H (ΔH_{acid} = 343.5 kcal mol^{-1}). The most basic site of tautomer **1a** is the N1 (PA = 228.4 kcal mol^{-1}).

ii. Experiments: Z acidity—We measured the acidity of Z using acidity bracketing (details in the Experimental Section). The conjugate base of Z deprotonates butyric acid (ΔH_{acid} = 346.8 ± 2.0 kcal mol^{-1}); the reaction in the opposite direction (butyrate with Z) also occurs (Table 1). We therefore bracket the ΔH_{acid} of Z as 347 ± 3 kcal mol^{-1}.

iii. Experiments: Z proton affinity—In bracketing the PA of Z, we find that piperidine (PA = 228.0 ± 2.0 kcal mol^{-1}) deprotonates protonated Z; the opposite reaction (Z deprotonating protonated piperidine) also occurs (Table 2). We therefore bracket the PA of Z to be 228 ± 3 kcal mol^{-1}.

3-deazaadenine (Z3, 2)

i. Calculations: Z3 tautomers, acidity, proton affinity—Z3 has seven possible tautomers, of which the most stable is the canonical "N9H" structure **2a** (Figure 4). The "N7H" tautomer **2b** is predicted to be 4 kcal mol^{-1} less stable than **2a**. The gas phase acidity of **2a** is 335.3 kcal mol^{-1} (corresponding to the N9-H). The most basic site of that tautomer is the N1, with a calculated PA of 233.2 kcal mol^{-1}.

ii. Experiments: Z3 acidity—The acidity of Z3 was measured using the bracketing method (Table 3). We find that deprotonated Z3 is able to deprotonate 2-chloropropanoic acid (ΔH_{acid} = 337.0 ± 2.1 kcal mol^{-1}). The reaction in the opposite direction (2-chloropropanoate with Z3) also occurs; we therefore bracket the ΔH_{acid} of Z3 to be 337 ± 3 kcal mol^{-1}.

iii. Experiments: Z3 proton affinity—The results for the bracketing of the PA of Z3 are in Table 4. We find that di-*sec*butylamine (PA = 234.4 ± 2.0 kcal mol^{-1}) is able to deprotonate protonated Z3, but that the opposite reaction (protonated di-sec-butylamine with Z3) does not occur. 1-Methylpiperidine (PA = 224.7 ± 2.0 kcal mol^{-1}) can *not* deprotonate protonated Z3, but Z3 can deprotonate protonated 1-methylpiperidine. We therefore bracket the PA of Z3 to be 233 ± 3 kcal mol^{-1}.

1-Deazaadenine (Z1, 3)

i. Calculations: Z1 tautomers, acidity, proton affinity—Z1 has seven possible tautomeric structures (Figure 5). The most stable tautomer (**3a**) is over 6 kcal mol^{-1} more stable than the next most stable species. The most acidic site of **3a** is predicted to be the N9 proton (ΔH_{acid} = 340.6 kcal mol^{-1}). The most basic site of tautomer **3a** is the N3 (PA = 230.0 kcal mol^{-1}).

ii. Experiments Z1 acidity—Efforts to sublime Z1 into the gas phase for acidity and proton affinity bracketing were unsuccessful; we failed to see signal corresponding to the substrate. We were, however, able to measure the acidity and proton affinity using an alternate method to bracketing, the "Cooks kinetic method" (details on this method in the Experimental Section). For the acidity measurement, five reference acids were used: 2-fluorobenzoic acid (ΔH_{acid} = 338.0 ± 2.2 kcal mol^{-1}), 3-hydroxybenzoic acid (ΔH_{acid} = 338.6 ± 2.1 kcal mol^{-1}), benzoic acid (ΔH_{acid} = 340.2 ± 2.2 kcal mol^{-1}), phenylacetic acid

(ΔH_{acid} = 341.5 ± 2.1 kcal mol^{-1}), and glycine (ΔH_{acid} = 342.7 ± 2.2 kcal mol^{-1}), yielding an acidity (ΔH_{acid}) of 341 ± 3 kcal mol^{-1}.

iii. Experiments: Z1 proton affinity—We were unable to measure Z1 PA by bracketing (vide supra), but were able to successfully utilize the Cooks kinetic method. Using guanine (PA = 229.3 ± 2.0 kcal mol^{-1}), *N*-methylpyrrolidine (PA = 230.8 ± 2.0 kcal mol^{-1}), 2,4-lutidine (PA = 230.1 ± 2.0 kcal mol^{-1}), dimethylisopropylamine (PA = 232.0 ± 2.0 kcal mol^{-1}), *N*-methylpiperidine (PA = 232.1 ± 2.0 kcal mol^{-1}), and triethylamine (PA = 234.7 ± 2.0 kcal mol^{-1}) as reference bases, we measure a PA for Z1 of 232 ± 3 kcal mol^{-1}.

"6-methylated" 1-deazaadenine (Q, 4)

i. Calculations: Q tautomers, acidity, proton affinity—There are three possible tautomeric structures for Q (Figure 6). The most stable tautomer **4a** is just over 4 kcal mol^{-1} more stable than the next most stable structure. The most acidic site of **4a** is the N9-H, with a ΔH_{acid} of 338.4 kcal mol^{-1}. The most basic site is the N7, with a PA of 223.0 kcal mol^{-1}.

ii. Experiments: Q acidity—The acidity of Q was bracketed as shown in Table 5. The reaction of deprotonated Q with methyl cyanoacetate (ΔH_{acid} = 340.80 ± 0.60 kcal mol^{-1}) occurs, as does the reverse reaction (deprotonated methyl cyanoacetate with Q). We therefore bracket the acidity of Q as 341 ± 2 kcal mol^{-1}.

iii. Experiments: Q proton affinity—The proton affinity of Q was bracketed as shown in Table 6. The results are somewhat unusual, in that reaction was found to occur in both directions for reference bases with PAs between 1-methylpyrrolidine (230.8 ± 2.0 kcal mol^{-1}) and pyridine (223.8. ± 2.0 kcal mol^{-1}). The implications of this will be addressed in the Discussion.

"6-methylated" 1,3,7-deazaadenine (M, 5)

i. Calculations: M tautomers, acidity, proton affinity—There are two possible tautomeric structures for M, with the more stable being so by over 7 kcal mol^{-1} (Figure 7). The more stable tautomer **5a** has a calculated acidity (at the most acidic site, the N9-H) of 347.9 kcal mol^{-1}. The PA of the most basic site, the C7, is 215.7 kcal mol^{-1}.

ii. Experiments: M acidity—Bracketing experiments with M were hindered by the inability to see any mass spectrometric signal when solid M is heated. However, we were able to vaporize (via electrospray) proton-bound dimers of M with reference acids, allowing us to measure the acidity of M via the Cooks kinetic method. Four reference acids were used (resorcinol (ΔH_{acid} = 346.6 ± 2.1 kcal mol^{-1}), propanoic acid (ΔH_{acid} = 347.4 ± 2.2 kcal mol^{-1}), imidazole (ΔH_{acid} = 349.9 ± 0.7), and 3-aminophenol (ΔH_{acid} = 350.5 ± 2.1 kcal mol^{-1})), yielding an acidity (ΔH_{acid}) of 349 ± 3 kcal mol^{-1}.

iii. Experiments: M proton affinity—As noted above, bracketing experiments with M were unsuccessful. In addition, measurement of the PA of M by the Cooks kinetic method also failed, as we were unable to form robust signal for proton-bound dimers with reference bases.

"6-methylated" 1,3-deazaadenine (B, 6)

i. Calculations: B tautomers, acidity, proton affinity—B has two possible tautomers, both of which are relatively close in stability (Figure 8). The most acidic site of the more stable tautomer **6a** is the N9-H (ΔH_{acid} = 339.4 kcal mol^{-1}). The most basic site is the N7, with a calculated PA of 228.2 kcal mol^{-1}.

ii. Experiments: B acidity—The acidity of B was bracketed as shown in Table 7. The reaction of deprotonated B with methyl cyanoacetate (ΔH_{acid} = 340.80 ± 0.60 kcal mol^{-1}) occurs; however, deprotonated methyl cyanoacetate cannot deprotonate B. Deprotonated B cannot deprotonate 2,4-pentadione (ΔH_{acid} = 343.8 ± 2.1 kcal mol^{-1}), but deprotonated 2,4-pentadione does deprotonate B. We therefore bracket the acidity of B to be 343 ± 3 kcal mol^{-1}.

iii. Experiments: B proton affinity—The PA of B was measured using bracketing (Table 8). We find that the reaction with piperidine (PA = 228.0 ± 2.0 kcal mol^{-1}) occurs in both directions (piperidine deprotonates protonated B, and B deprotonates protonated piperidine). We therefore measure the PA of B as 228 ± 3 kcal mol^{-1}.

MutY-catalyzed base excision

Most of the unnatural adenine analogs studied herein (Z, Z3, Q, B, M) have previously been examined as substrates for MutY in DNA duplexes base-paired opposite OG, in order to probe enzymatic mechanistic features.[25-28] However, the modified Z1 duplex substrate had not been previously examined and is not commercially available. The appropriate monomer for automated DNA synthesis was synthesized and incorporated into a 30-nucleotide strand (Supplementary Information). The glycosylase activity of MutY on a 30-bp duplex containing a central OG:X (X = adenine or adenine analog) was evaluated as previously reported.[33] Briefly, this involves analyzing the extent of strand scission as a function of time after NaOH quenching of reaction mixtures. Reaction rate constants (k_g) were measured under conditions of single-turnover ([MutY] > [DNA substrate]) to remove complications associated with rate-limiting product release. In the case of the OG:Z1-containing duplex, the measured rate constant at 37 °C is 0.3 ± 0.1 min^{-1}. This represents a 40-fold decrease under the same conditions for the reaction of MutY with the corresponding OG:A-containing substrate (k_g = 12 ± 2 min^{-1}). For the series of adenine analog substrates, the MutY glycosylase activity (k_g), relative to A, is shown in Table 9 (in decreasing order). The substrates are cleaved by MutY in the order: A>Q>Z1>Z3>B>>M=Z.

Acid-catalyzed depurination of A analog-containing DNA

Previous work has shown that comparing MutY rates to the susceptibility for acid-catalyzed depurination can reveal insight into features of the enzyme-catalyzed rate. Indeed, previous work with the hydrophobic analogues, B and Q, showed that these analogs are more susceptible to depurination than A.[25] The relative acid-catalyzed depurination of Z1 and Z3 relative to A in the 30 nt oligonucleotide was evaluated using a modified Maxam Gilbert G +A reaction (Supplementary Information). The extent of depurination was quantitated using autoradiography (Figure S1, Supporting Information) and the relative extents of

depurination of Z1, Z3 and A were normalized to depurination of another A (position 11) within the DNA sequence (Figure S2, Supporting Information). These results show that A, Z1, and Z3 at position 15 are depurinated at fractions of 0.9, 6.3, and 0.3 relative to A11 in the same DNA sequence. Interestingly, this shows that in contrast to the enzyme-catalyzed excision rates, in acidic water Z1 is depurinated seven times more than A whereas depurination of Z3 is three times less efficient (Table 10). The trend for acid-catalyzed depurination is: Q=Z1>B>A>Z3.

Discussion

Calculated versus experimental values

The calculated acidity and proton affinity values for all the substrates studied herein are summarized in Table 11. (Adenine was previously measured and calculated by us and also appears in the Table). Generally, B3LYP/6-31+G(d) appears to provide fairly accurate predictions for the thermochemical values. The one instance where the calculated and experimental data are quite disparate is for the proton affinity of Q: the calculated value for the most stable tautomer is 223.0 kcal mol^{-1} yet the bracketing experiment yields a wide range where proton transfer occurs in both directions (PAs from 223.8 to 230.8 kcal mol[1], Table 6). This is a fairly significant discrepancy.

The wide range of proton transfer in both directions for the PA bracketing of Q (Table 6) raises the possibility that under our conditions, we have a mixture of the two most stable Q tautomers (**4a** and **4b**), and the more basic **4b** (calculated PA of 232.6 kcal mol^{-1}) influences the experimentally observed value. Although the B3LYP/6-31+G(d) calculations indicate that **4b** is nearly 5 kcal mol^{-1} less stable than **4a**, prior studies show that accurate calculations of nucleobase tautomer stabilities can be elusive.[35-39] It is possible that **4b** is less stable than **4a** but perhaps not by as much as the calculations indicate, such that there is some **4b** present in our experiments.

For the PA bracketing experiment, the solid **4** is sublimed into the gas phase via a solids probe (typical pressure in the instrument is 10^{-7} to 10^{-8} Torr, and the probe is heated to a temperature of roughly 400K). If only **4a** were present, one would expect a bracketed PA of around 223 kcal mol^{-1}, based on the calculations (Figure 6, Table 11). The bracketing table would have a “crossover” point near pyridine (Table 12).

If only **4b** were present, one would expect a similar table, except the “crossover point” would be near the PA of the most basic site of **4b**, which is calculated to be 232.6 kcal mol^{-1} (Figure 6). Instead, as can be seen in Table 6, there is not a clean crossover point, but rather a range in which the deprotonation reaction occurs in both directions. We suspect that the reason for this is that both tautomers **4a** and **4b** are present.

In the reactions of a reference base with protonated **4**, if both tautomers were present, then the protonated substrate should be a mixture of $\mathbf{4aH^+}$ and $\mathbf{4bH^+}$ (Figure 9). Under these conditions, any reference base with a proton affinity greater than or equal to 223.0 kcal mol^{-1} should deprotonate **4a**. Consistent with this expectation, we do observe proton

transfer for all the reference bases from 3-picoline (PA = 225.5 kcal mol^{-1}) to 1-methylpiperidine (PA = 232.1 kcal mol^{-1}, Table 6, "Ref. base" column).

In the opposite direction, the protonated reference bases are allowed to react with **4.** If both **4a** and **4b** are present, we would expect reaction with any protonated reference base with a PA of about 232 kcal mol^{-1} or less, because **4b** has a calculated PA of 232.6 kcal mol^{-1} (Figure 9). We actually see proton transfer "turn on" at a slightly lower value, 228.0 kcal mol^{-1} (at piperidine; Table 6, "Conj. acid" column). Still, this value is much higher than the calculated PA of **4a** (223.0 kcal mol^{-1}), pointing to the probable presence of **4b**.

We suspect that the proton transfer "turning on" at a slightly lower value than calculated may be due to a mixture in which **4a** predominates, with less of **4b.** In this bracketing experiment, in order to ascertain whether proton transfer occurs, we measure the kinetics of the proton transfer. We track the disappearance of the protonated reference base signal under pseudo-first order conditions (excess of **4**). We can measure the pressure of **4**, but do not know what percentage is **4b** versus **4a**. Therefore, for those protonated reference bases that only react with **4b**, we measure a rate constant for proton transfer that is less than the actual rate constant, because we can only measure the overall pressure of **4**, but only **4b** reacts. Our PA bracketing results are therefore consistent with a mixture of **4a** and **4b**, with **4a** predominating.

We should also address the bracketed acidity measurement of Q. Tautomer **4a** has a calculated acidity of 338.4 kcal mol^{-1}; tautomer **4b**, 333.8 kcal mol^{-1}. The measured value is 341 kcal mol^{-1}, which implies the presence of tautomer **4a** but not **4b.** However, as we discuss above, we believe both tautomers are present. So why do we measure an acidity consistent with **4a** only?

The deprotonation of both **4a** and **4b** results in the same anion, which is allowed to react with reference acids (Figure 10). This anion should be able to deprotonate any reference acid with ΔH_{acid} of ~338 kcal mol^{-1} or less. Experimentally, we do see proton transfer "turn on" in this region, starting with methyl cyanoacetate (ΔH_{acid} = 340.8 kcal mol^{-1}, Table 5 ("Ref. acid" column)).

In the opposite direction, deprotonated reference acids would be allowed to react with **4**, which is presumably a mixture of **4a** and **4b** (Figure 11). In this direction, one would expect to see reaction with any deprotonated reference acid whose ΔH_{acid} is 334 kcal mol^{-1} or higher (since **4b** is present). Instead, however, we do not see proton transfer "turn on" until 340.8 kcal mol^{-1} (Table 5, "Conj. base" column). We believe that two factors are at play: one, as we saw with the PA experiments, we have less **4b** present, so reactions with **4b** will appear slower than they are. Second, we cannot preclude base-catalyzed tautomerization of **4b** to **4a** taking place during the bracketing experiment (Figure 12; brackets indicate ion-molecule complexes; A^- is the deprotonated reference acid). In Figure 12, we show the reaction of a deprotonated reference acid A^- with **4b**. In this Figure, the reference acid has a ΔH_{acid} of 336 kcal mol^{-1}, which is a higher value than the ΔH_{acid} of **4b**, so proton transfer occurs to form deprotonated **4**. However, if a subsequent proton transfer takes place (whereby the $N9^-$ of deprotonated **4**, whose conjugate acid has an acidity of 338.4 kcal

mol^{-1}, deprotonates AH), then **4a** and A$^-$ are formed as products (Figure 12). Proton transfer between **4b** and A$^-$ has occurred, but since we only track the m/z ratio of A$^-$, we would have no way of knowing that proton transfer occurred. The exothermic scenario shown in Figure 12 would look, by mass spectrometry, as if no proton transfer has taken place: one would only see A$^-$ signal when following the reaction progress. This would therefore be marked as a "–" in the last column of Table 5, even though proton transfer has occurred. Essentially, therefore, the "–" entries in the rightmost column of Table 5 may actually be incorrect. Thus, the bracketed ΔH_{acid} value of 341 kcal mol^{-1} does not necessarily mean that **4b** is not present.

Given the wide range of proton transfer in both directions for the PA experiment (Figure 6) and the ambiguity associated with knowing whether proton transfer occurred in the acidity experiment, we therefore believe that we most likely have a mixture of **4a** and **4b** present under our experimental conditions, with **4a** predominating.

Biological implications

MutY is a glycosylase that cleaves adenine when it is base-paired to OG. The unnatural substrates studied herein (Z, Z3, Z1, Q, B, M) were synthesized and examined as substrates for MutY, in order to probe enzymatic mechanistic features (most in prior work).[25-28] The rates of excision, relative to A, are shown in Table 9 (in decreasing order). The substrates are cleaved by MutY in the order: A>Q>Z1>Z3>B>>M=Z.

As a key step in initiating DNA repair, BER glycosylases, such as MutY, cleave the *N*-glycosidic bond (Figure 1) to release the damaged or inappropriate base. MutY is a monofunctional glycosylase that hydrolyzes the N-glycosidic bond on 2'-deoxyadenosine to yield an abasic site-DNA product and free adenine base. We are interested in whether the intrinsic properties that we study herein can lend insight into the features used by MutY to catalyze *N*-glycosidic bond breakage. Presumably, the better a leaving group the nucleobase is, the more easily it is cleaved. Since acidity and leaving group ability are generally correlated, we would expect more easily cleaved bases to be more acidic. By examining the intrinsic N9-H bond stability for various possible mechanisms, we can lend insight into the operative mechanism. Furthermore, based on our studies with other glycosylases, we postulate that MutY may provide a nonpolar active site that serves to *enhance* the differences in acidity among nucleobases, and in doing so, aids in the discrimination of substrate bases over nonsubstrate bases.[18,19,21,23,40] Thus, studies in the gas phase, which is the ultimate nonpolar environment, are relevant.

Mechanistic studies of MutY, including crystal structure, KIE studies, and computer (molecular dynamics and QM/MM) simulations point to protonation at N7 to facilitiate cleavage.[14-17,41] A recent crystal structure of *Bacillus stearothermophilus* MutY bound to a DNA duplex containing a fluorinated 2'-deoxyadenosine paired with OG shows multiple hydrogen bonding contacts as well as hydrophobic interactions between substrate and enzyme.[14,16,41] Glu-43 and Tyr-126 coordinately contact the N7; the position of the glutamate indicates that it is probably protonated (the carboxylic acid as opposed to the carboxylate). Glu43 is expected to be quite acidic, allowing partial or full bonding of its proton to N7. A hydrogen bond from Arg-26 to water to N3 is observed, as well as a

hydrogen bond from Arg-31 to N1. Various salt bridges exclude water and create a hydrophobic environ.[14,16,25-27]

Acidity: N9-H acidity of neutral nucleobase analogs

First we considered a mechanism where the *N*-glycosidic bond is simply cleaved without any pre-protonation; in such a scenario, the leaving group is a deprotonated anion (Mechanism A, Scheme 1). In this case, the acidities of the neutral substrates will correlate to their leaving group abilities. The calculated (B3LYP/6-31+G(d)) values for the N9-H acidity for the neutral nucleobase analogs are shown in Figure 13. Lower values are more acidic, so adenine is the most acidic substrate (ΔH_{acid} of 334.8 kcal mol^{-1}).[21,22,39,42-47] The next most acidic substrate is Z3 (ΔH_{acid} = 335.3 kcal mol^{-1}). (Substrates are ordered in increasing acidity). The trend from most to least acidic in the gas phase is: adenine (A)>Z3>Q>B>Z1>Z>M (where A is most acidic). This trend does not agree with the known excision rates for these substrates by MutY (Table 9), which is A>Q>Z1>Z3>B>>M=Z. Furthermore, the acidity values for Z and M do not seem high enough (relative to the other nucleobases) to explain the experimentally observed lack of excision. Thus, a mechanism where the nucleobases are simply cleaved as anions seems unlikely, at least based on the intrinsic acidity of these substrates. This is not too surprising, since most experimental evidence points to pre-protonation at N7 (Mechanism B, Scheme 1).

Acidity: N9-H acidity of N7-protonated substrates

The N9-H acidity values for the N7-protonated nucleobase analogs are shown in Figure 14 (listed in order of increasing acidity). N7-Protonation greatly increases the N9-H acidity (by more than 100 kcal mol^{-1}). The acidity trend is: A~Z3>Q>B>Z1>>Z>M. (The acidities of Z and M without protonation are shown since they lack an N7).

The acidity trend, at first glance, does not correlate to the known excision rates for these substrates by MutY (Table 9, A>Q>Z1>Z3>B>M=Z) . However, there are some consistencies. M and Z, because of the inability to protonate at N7, are the least acidic by far and would not expect to be prone to cleavage, which is what is observed experimentally. Q and Z1 are more easily cleaved than would be predicted by the acidities in Figure 14, but both have one feature in common: a nitrogen at N3, which has been proposed to be important for MutY excision.[14,16,25,26]

In order to model the effect of acidity by hydrogen bonding at N3, we used HF as a simple hydrogen bonding donor.[48] The hydrogen bond at N3 increases the acidity at the N9-H of the N7-protonated substrates by roughly 2-3 kcal mol^{-1}. In Figure 15, we show the gas phase acidities of the substrates protonated at N7 and hydrogen bonded to N3 (when the N is present at the 7 and 3 positions). The resultant acidity trend is: A>Z3~Q>Z1>B>>Z>M.

This trend compares quite favorably to the actual MutY excision rates (Table 9, A>Q>Z1>Z3>B>M=Z). The only substrate “out of place” is the Z3, whose gas phase acidity when protonated at N7 is quite high and implies that Z3 should be prone to cleavage. The reduced ability of MutY to remove Z3 is somewhat of a mystery from the experimental point of view as well; in earlier work one of us postulated that the lack of a N at the 3-

position might render the N7 more difficult to protonate, which could reduce excision rate. Our gas phase PA calculations do indicate that Z3 is less basic at N7 than Q and Z1 (Figure 16), so this may explain the observed excision trend.[25-28]

Thus, the gas-phase N9-H acidities of these substrates can be compared to known excision rates to lend insight into the MutY mechanism. The gas-phase acidities of the substrates track with excision rates when the N7 is protonated and a hydrogen bond is formed to the N3, implying that these are features that MutY may provide to enable nucleobase cleavage.

Acid-catalyzed non-enzymatic depurination

We have also studied the nonenzymatic excision of some of these nucleobase analogs in acidic aqueous solution and find a different trend than that for MutY-catalyzed excision. B, Q and Z1 are depurinated more quickly than A while Z3 is depurinated more slowly (Q=Z1>B>A>Z3, Table 10).[25] Because this excision trend is different from that catalyzed by MutY, we postulate that the mechanism in acidic aqueous solution is different. Presumably, under acidic conditions, the most basic site of a given nucleobase analog is protonated, which favors cleavage of the nucleobase. Since the most basic site is not always N7, the acidic aqueous mechanism is different from that of MutY.

To mimic these conditions, relevant calculations should involve pre-protonation of the most basic site and a polar environment. To that end, we calculated the N9-H acidity for the nucleobase analogs when the most basic site is protonated, in a water dielectric (Figure 17). The acidity values are much lower than those in the gas phase, as would be expected in water. These calculations indicate an N9-H acidity trend of: Q>B>Z1>A>Z3. We would therefore expect Q, B and Z1 to be cleaved more quickly than adenine, and Z3 to be cleaved more slowly, which is consistent with the experimental results (Table 10). The calculations, which do not include specific solvation, are not perfect; B is predicted to be more quickly cleaved than Z1 but experimentally the opposite is observed. However, the overall trend of which bases should be cleaved more quickly than A and which less quickly is consistent between calculations and experiment, supporting a mechanism in which acid pre-protonates the most basic site prior to cleavage.

1,3-deazaadenine (Z13) prediction

One additional substrate we studied computationally is Z13 (Figure 18). This is a logical extension of the various analogs already studied (Figure 2); this particular derivative is missing an “N” at both the 1 and 3 positions. Z13 could be a substrate for MutY, although the only nitrogen available for hydrogen bonding and/or protonation is the N7. Compared to the other nucleobase analogs, the acidity at N9-H when that N7 is protonated is fairly poor (ΔH_{acid} = 230.1 kcal mol^{-1}). Given our hypothesis that the N7 is protonated and the N3 is hydrogen bonded, the acidity of the N9-H of Z13 is even less than that of B (Figure 15). We would therefore expect Z13 to be cleaved by MutY quite slowly, even more slowly than B (but still faster than Z or M) .

Conclusions

The heretofore unknown thermochemical properties of adenine and six adenine analogs have been calculated and measured herein. Gas phase measurements benchmark our calculations. Comparison of the stability of the N9-H bond (in terms of acidity) versus known MutY excision rates point to a MutY-catalyzed mechanism involving protonation at N7, with hydrogen bonding at N3. This conclusion is consistent with other MutY mechanistic studies (crystal structures, kinetic isotope effects). We also find that our calculations for the N9-H acidity when the most basic site is protonated are consistent with experimental data for acid-catalyzed depurination in water. Our work shows that fundamental studies of biological species are valuable for lending insight into mechanisms for which these species are substrates.

Experimental

All of the nucleobase analogs (except Z1) and reference acids and bases are commercially available and were used as received. Synthesis of 1-deazaadenosine (Z1) and Z1-containing oligonucleotides was similar to methods previously described; additional details are in the Supporting Information.[49] Adenine glycosylase assays and acid-catalyzed depurination reactions were also performed as described previously; additional details are provided in the Supporting Information.[25]

The bracketing method was used to measure the gas phase acidity and proton affinity values. A Fourier transform ion cyclotron resonance mass spectrometer (FT-ICR) with dual cell setup (described previously) was used.[18,19,21,34,50] The magnetic field is 3.3 T; the baseline pressure is 1×10^{-9} Torr. The solid nucleobase analogs were introduced into the cell via a heatable solids probe, while liquid reference acids and bases were introduced via a system of heatable batch inlets. Water was pulsed into the cell, and ionized by an electron beam (typically 8 eV (for HO^-), 20 eV (for H_3O^+), 6 μA, 0.5 s) to generate hydroxide and hydronium ions. Substrate ions were generated by deprotonation or protonation of reference acids or bases (with hydroxide or hydronium ions, respectively), then selected, and transferred from one cubic cell to another via a 2-mm hole in the middle trapping plate. Transferred ions were cooled with pulsed argon gas that allowed the pressure to rise to 10^{-5} Torr. Experiments were conducted at ambient temperature.

The typical protocol for bracketing experiments has been described previously.[18,19,29,30,50] Proton transfer reactions were conducted in both directions. For example, for Z3 acidity bracketing, hydroxide is used to deprotonate neutral Z3. Deprotonated Z3 is transferred into the adjoining cell where it is allowed to react with the neutral reference acid AH with known gas phase acidity. In the opposite direction, the deprotonated reference acid A^- is generated and transferred into the adjoining cell where it is allowed to react with neutral Z3. The occurrence of proton transfer is regarded as evidence that the reaction is exothermic (denoted as "+" in the tables). Bracketing experiments are run under pseudo-first-order conditions with the neutral reactant in excess, relative to the reactant ions. Reading the pressure of the neutral compounds from the ion gauges is not always accurate; therefore, we

"back out" the neutral substrate pressure from fast control reactions (described previously).[19,22,23,30,51,52]

We also utilized the Cooks kinetic method in a quadrupole ion trap (LCQ) mass spectrometer[53-56] to measure the acidities and proton affinities of adenine analogs. The Cooks kinetic method involves the formation of a proton-bound complex, or dimer, of the unknown and a reference acid or base of known acidity or PA.

The proton-bound dimer ions are generated by electrospray (ESI) of 250 μM solutions of an unknown and a reference acid (or base, for PA measurement). Water–methanol (20%) solution is used as solvent.[57] One drop of acetic acid (for PA measurements) or ammonium hydroxide (for acidity measurements) is occasionally used to promote dimer formation. An electrospray needle voltage of ~4 kV and a flow rate of 25 μL/min is applied. The proton-bound complex ions are isolated and then dissociated by applying collision-induced dissociation (CID); the complexes are activated for about 30 ms. Finally, the dissociation product ions are detected to give the ratio of the deprotonated (or protonated) analyte and deprotonated (or protonated) reference acid. A total of 40 scans are averaged for the product ions.

The dissociation of the proton bound dimer $[AHB_i]^-$ is depicted in Eq. 1 (where AH is the compound of unknown acidity and B_iH represents a series of reference acids of known acidity). The rate constants k_1 and k_2 are for the two different dissociation pathways.

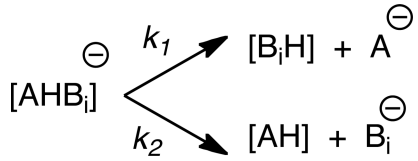

(Eq. 1)

$$ln\,(k_1/k_2) = (1/RT_{eff})\,(\Delta H_{BIH} - \Delta H_{AH}) \quad \text{(Eq. 2)}$$

The relationship of these rate constants to ΔH_{acid} is shown in Eq. 2, where R is the gas constant and T_{eff} is the effective temperature[58] of the activated dimer.[53-56] The ratio of the intensities of the two deprotonated products yields the relative acidity of the two compounds of interest (Eq. 2), assuming the dissociation has no reverse activation energy barrier and that the dissociation transition structure is late (and therefore indicative of the stability of the two deprotonated products). These assumptions are generally true for proton bound systems.[56,59,60]

In order to obtain the acidity of compound AH, the natural logarithm of the relative intensity ratios is plotted versus the acidities for a series of reference acids (B_iH), where the slope is ($1/RT_{eff}$) and the y-intercept is ($-\Delta H_{AH}/RT_{eff}$). The T_{eff} is obtained from the slope. The acidity of compound AH, (ΔH_{AH}) is calculated from either Eq. 2 or the y-intercept. The

same procedure was applied for proton affinity measurements (via formation of positively charged proton bound dimers).

The gas phase calculations were conducted at the B3LYP/6-31+G(d) level using Gaussian03 and Gaussian09.[61-65] All the structures were fully optimized in the gas phase, and frequencies calculated (no imaginary frequencies were found). Acidity and proton affinity values are reported as ΔH at 298 K.

Dielectric medium calculations were done using the conductor-like polarizable continuum solvent model (CPCM, single point calculations on B3LYP/6-31+G(d) gas phase optimized structures; UAKS cavity) at B3LYP/6-31+G(d) as implemented in Gaussian03.[66,67,68] The "total free energy in solution" values are reported, and the solvation free energy of a proton (-264.0 kcal mol^{-1}) is accounted for.[69,70]

Supplementary Material

Refer to Web version on PubMed Central for supplementary material.

Acknowledgments

We gratefully thank the NSF, ACS-PRF, NCI/NIH (CA67985) and the National Center for Supercomputer Applications for support.

REFERENCES

1. David SS, Williams SD. Chem. Rev. 1998; 98:1221–1261. [PubMed: 11848931]
2. Lindahl T. Nature. 1993; 362:709–715. [PubMed: 8469282]
3. Klaunig JE, Kamendulis LM. Annu. Rev. Pharmacol. Toxicol. 2004; 44:239–267. [PubMed: 14744246]
4. Neeley WL, Essigmann JM. Chem. Res. Toxicol. 2006; 19:491–505. [PubMed: 16608160]
5. Shigenaga MK, Park J-W, Cundy KC, Gimeno CJ, Ames BN. Methods Enzymol. 1990; 186:521–530. [PubMed: 2233317]
6. Dizdaroglu M. Biochemistry. 1985; 24:4476–4481. [PubMed: 4052410]
7. Burrows CJ, Muller JG. Chem. Rev. 1998; 98:1109–1152. [PubMed: 11848927]
8. McAuley-Hecht KE, Leonard GA, Gibson NJ, Thomson JB, Watson WP, Hunter WN, Brown T. Biochemistry. 1994; 33:10266–10270. [PubMed: 8068665]
9. Cunningham RP. Mutat. Res. 1997; 383:189–196. [PubMed: 9164479]
10. Michaels ML, Tchou J, Grollman AP, Miller JH. Biochemistry. 1992; 31:10964–10968. [PubMed: 1445834]
11. David SS, O'Shea VL, Kundu S. Nature. 2007; 447:941–950. [PubMed: 17581577]
12. Michaels ML, Miller JH. J. Bacteriol. 1992; 174:6321–6325. [PubMed: 1328155]
13. Michaels ML, Cruz C, Grollman AP, Miller JH. Proc. Natl. Acad. Sci. 1992; 89:7022–7025. [PubMed: 1495996]
14. Lee S, Verdine GL. Proc. Natl. Acad. Sci. 2009; 106:18497–18502. [PubMed: 19841264]
15. McCann JAB, Berti PJ. J. Am. Chem. Soc. 2008; 130:5789–5797. [PubMed: 18393424]
16. Fromme JC, Banerjee A, Huang SJ, Verdine GL. Nature. 2004; 427:652–656. [PubMed: 14961129]
17. Brunk E, Arey JS, Rothlisberger U. J. Am. Chem. Soc. 2012; 134:8608–8616. [PubMed: 22537339]
18. Kurinovich MA, Lee JK. J. Am. Chem. Soc. 2000; 122:6258–6262.

19. Liu M, Xu M, Lee JK. J. Org. Chem. 2008; 73:5907–5914. [PubMed: 18593189]
20. Sun X, Lee JK. J. Org. Chem. 2010; 75:1848–1854. [PubMed: 20184296]
21. Sharma S, Lee JK. J. Org. Chem. 2002; 67:8360–8365. [PubMed: 12444612]
22. Zhachkina A, Liu M, Sun X, Amegayibor S, Lee JK. J. Org. Chem. 2009; 74:7429–7440. [PubMed: 19731957]
23. Sun X, Lee JK. J. Org. Chem. 2007; 72:6548–6555. [PubMed: 17655363]
24. Lee JK. Int. J. Mass Spectrom. 2005; 240:261–272.
25. Francis AW, Helquist SA, Kool ET, David SS. J. Am. Chem. Soc. 2003; 125:16235–16242. [PubMed: 14692765]
26. Livingston AL, O'Shea VL, Kim T, Kool ET, David SS. Nature Chem. Biol. 2008; 4:51–58. [PubMed: 18026095]
27. Chepanoske CL, Langelier CR, Chmiel NH, David SS. Org. Lett. 2000; 2:1341–1344. [PubMed: 10810743]
28. Porello SL, Williams SD, Kuhn H, Michaels ML, David SS. J. Am. Chem. Soc. 1996; 118:10684–10692.
29. Kurinovich MA, Lee JK. J. Am. Soc. Mass Spectrom. 2002; 13:985–995. [PubMed: 12216739]
30. Liu M, Li T, Amegayibor S, Cardoso DS, Fu Y, Lee JK. J. Org. Chem. 2008; 73:9283–9291. [PubMed: 18973382]
31. Linstrom, PJ.; Mallard, WG., editors. NIST Chemistry WebBook, NIST Standard Reference Database Number 69; retrieved in 2011. National Institute of Standards and Technology; Gaithersburg, MD: 20899, http://webbook.nist.gov.
32. Eyet N, Villano SM, Bierbaum VM. Int. J. Mass Spectrom. 2009; 283:26–29.
33. Porello SL, Leyes AE, David SS. Biochemistry. 1998; 37:14756–14764. [PubMed: 9778350]
34. Sharma S, Lee JK. J. Org. Chem. 2004; 69:7018–7025. [PubMed: 15471447]
35. Wolken JK, Yao C, Turecek F, Polce MJ, Wesdemiotis C. Int. J. of Mass Spectrom. 2007; 267:30–42.
36. Shukla MK, Leszczynski J. Chem. Phys. Lett. 2006; 429:261–265.
37. Plekan O, Feyer V, Richter R, Coreno M, Vall-llosera G, Prince KC, Trofimov AB, Zaytseva IL, Moskovskaya TE, Gromov EV, Schirmer J. J. Phys. Chem. A. 2009; 113:9376–9385. [PubMed: 19634878]
38. Trygubenko SA, Bogdan TV, Rueda M, Orozco M, Luque FJ, Sponer J, Slavicek P, Hobza P. Phys. Chem. Chem. Phys. 2002; 4:4192–4203.
39. Colominas C, Luque FJ, Orozco M. J. Am. Chem. Soc. 1996; 118:6811–6821. and references therein.
40. Bennett MT, Rodgers MT, Hebert AS, Ruslander LE, Eisele L, Drohat AC. J. Am. Chem. Soc. 2006; 128:12510–12519. [PubMed: 16984202]
41. Guan Y, Manuel RC, Arvai AS, Parikh SS, Mol CD, Miller JH, Lloyd RS, Tainer JA. Nat. Str. Biol. 1998; 5:1058–1064.
42. Podolyan Y, Gorb L, Leszczynski J. J. Phys. Chem. A. 2000; 104:7346–7352. and references therein.
43. Hanus M, Kabelac M, Rejnek J, Ryjacek F, Hobza P. J. Phys. Chem. B. 2004; 208:2087–2097.
44. Russo N, Toscano M, Grand A, Jolibois F. J. Comput. Chem. 1998; 19:989–1000.
45. Huang Y, Kenttämaa H. J. Phys. Chem. A. 2004; 108:4485–4490.
46. Chandra AK, Nguyen MT, Uchimaru T, Zeegers-Huyskens T. J. Phys. Chem. A. 1999; 103:8853–8860.
47. Del Bene JE. J. Phys. Chem. 1983; 87:367–371.
48. We also attempted to use water as the hydrogen bond donor, but calculations were complicated by the propensity of the water proton to hydrogen bond to N9 after deprotonation.
49. DeCarlo L, Prakasha Gowda AS, Suo Z, Spratt TE. Biochemistry. 2008; 47:8157–8164. [PubMed: 18616289]
50. Kurinovich MA, Lee JK. Chem. Commun. 2002:2354–2355.
51. Chesnavich WJ, Su T, Bowers MT. J. Chem. Phys. 1980; 72:2641–2655.

52. Su T, Chesnavich WJ. J. Chem. Phys. 1982; 76:5183–5185.
53. Cooks RG, Kruger TL. J. Am. Chem. Soc. 1977; 99:1279–1281.
54. McLuckey SA, Cameron D, Cooks RG. J. Am. Chem. Soc. 1981; 103:1313–1317.
55. McLuckey SA, Cooks RG, Fulford JE. Int. J. Mass Spectrom. and Ion Physics. 1983; 52:165–174.
56. Green-Church KB, Limbach PA. J. Am. Soc. Mass Spectrom. 2000; 11:24–32. [PubMed: 10631661]
57. Fenn JB, Mann M, Meng CK, Wong SF, Whitehouse CM. Science. 1989; 246:64–71. [PubMed: 2675315]
58. Drahos L, Vékey K. J. Mass Spectrom. 1999; 34:79–84.
59. Ervin KM. Chem. Rev. 2001; 101:391–444. [PubMed: 11712253]
60. Gronert S, Feng WY, Chew F, Wu W. Int. J. Mass Spectrom. 2000; 195/196:251–258.
61. Becke AD. J. Chem. Phys. 1993; 98:5648–5652.
62. Lee C, Yang W, Parr RG. Phys. Rev. B. 1988; 37:785–789.
63. Kohn W, Becke AD, Parr RG. J. Chem. Phys. 1996; 100:12974–12980.
64. Frisch, MJ., et al. Gaussian 03. Gaussian, Inc.; Wallingford CT: 2004.
65. Frisch, MJ., et al. Gaussian 09. Gaussian, Inc.; Wallingford CT: 2009.
66. Barone V, Cossi M. J. Phys. Chem. A. 1998; 102:1995–2001.
67. Cossi M, Rega N, Scalmani G, Barone V. J. Comp. Chem. 2003; 24:669–681. [PubMed: 12666158]
68. Takano Y, Houk KN. J. Chem. Theory Comput. 2005; 1:70–77.
69. Tissandier MD, Cowen KA, Feng WY, Gundlach E, Cohen MH, Earhart AD, Coe JV, Tuttle TR. J. Phys. Chem. A. 1998; 102:7787–7794.
70. Chipman DM. J. Phys. Chem. A. 2002; 106:7413–7422.

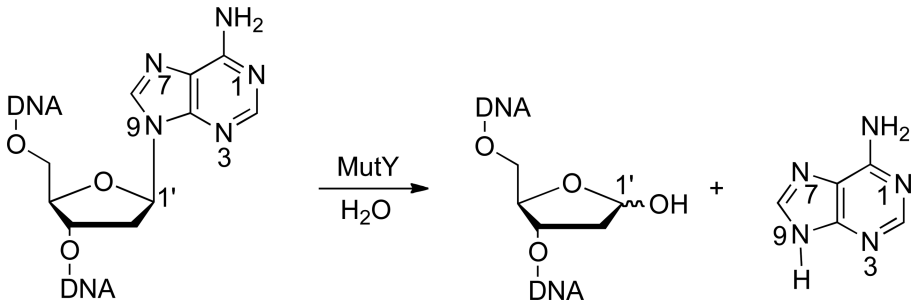

Figure 1.
Adenine removal from DNA catalyzed by the MutY glycosylase.

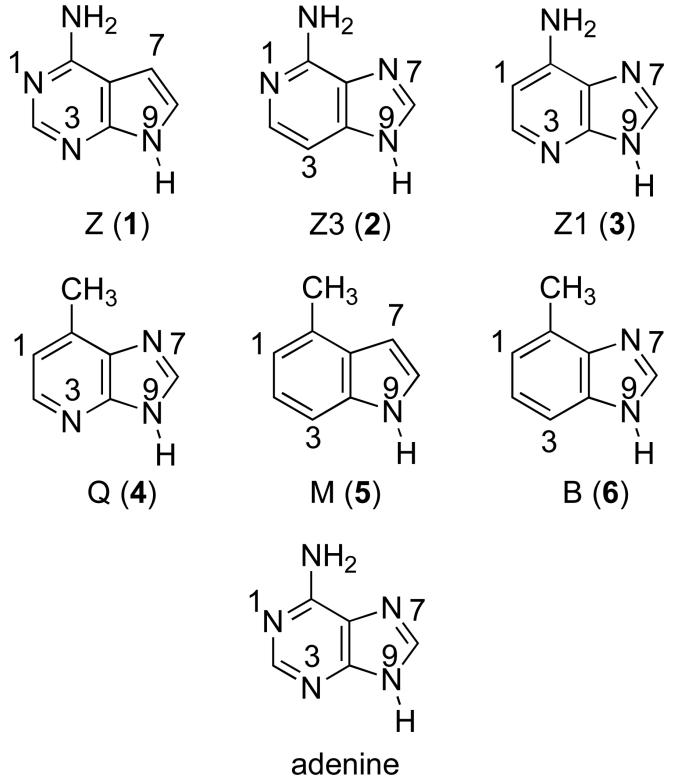

Figure 2.
Adenine and synthetic analogs studied herein.

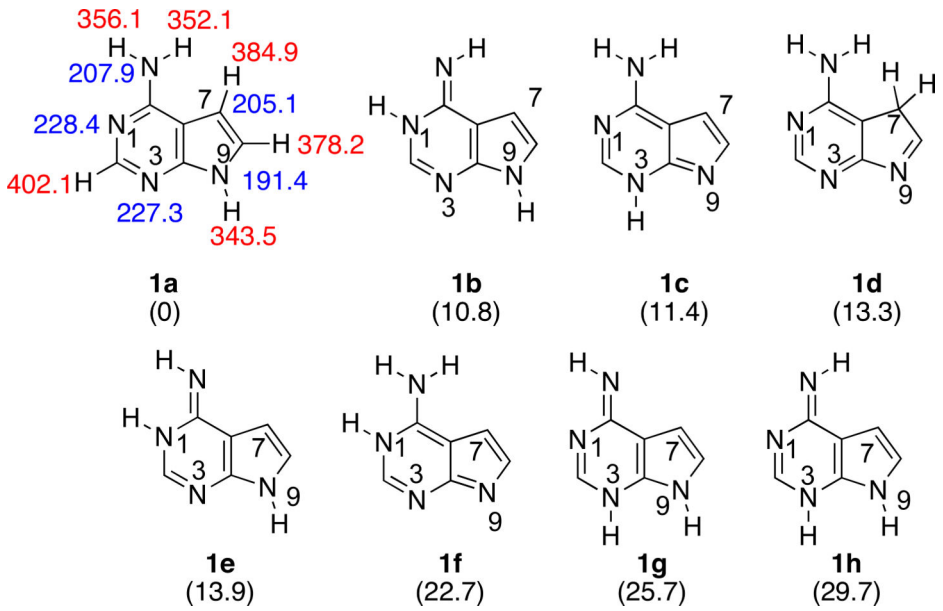

Figure 3.

The eight possible tautomeric structures of 7-deazaadenine (Z). Gas phase acidities are in red; gas phase proton affinities are in blue. Relative stabilities are in parentheses. Calculations were conducted at B3LYP/6-31+G(d); reported values are ΔH at 298 K.

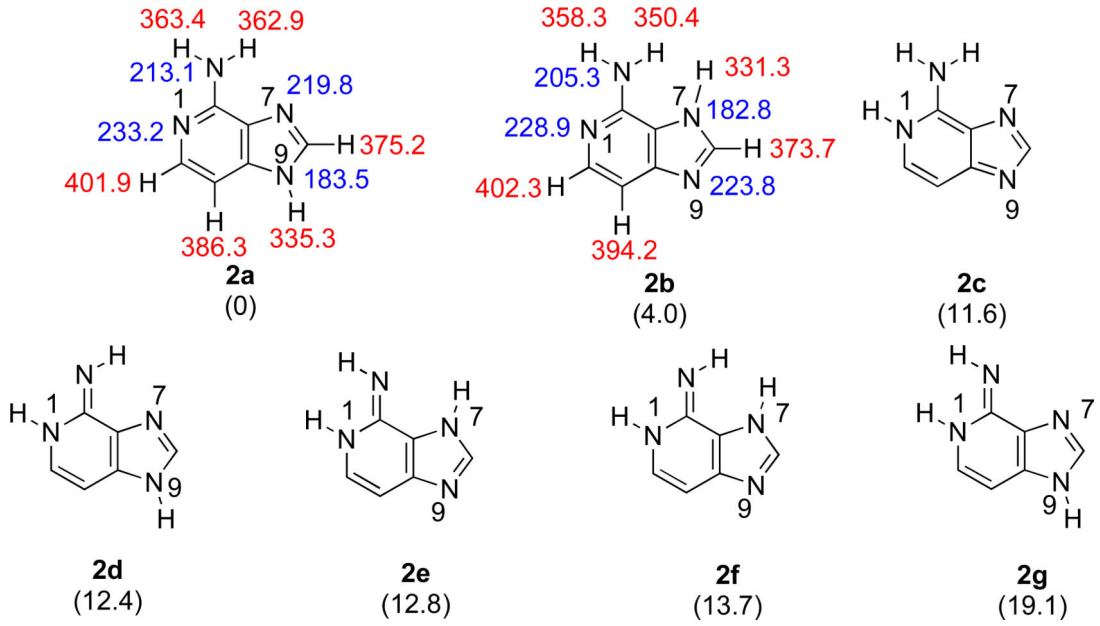

Figure 4.

The seven possible tautomeric structures of 3-deazaadenine (Z3). Gas phase acidities are in red; gas phase proton affinities are in blue. Relative stabilities are in parentheses. Calculations were conducted at B3LYP/6-31+G(d); reported values are ΔH at 298 K.

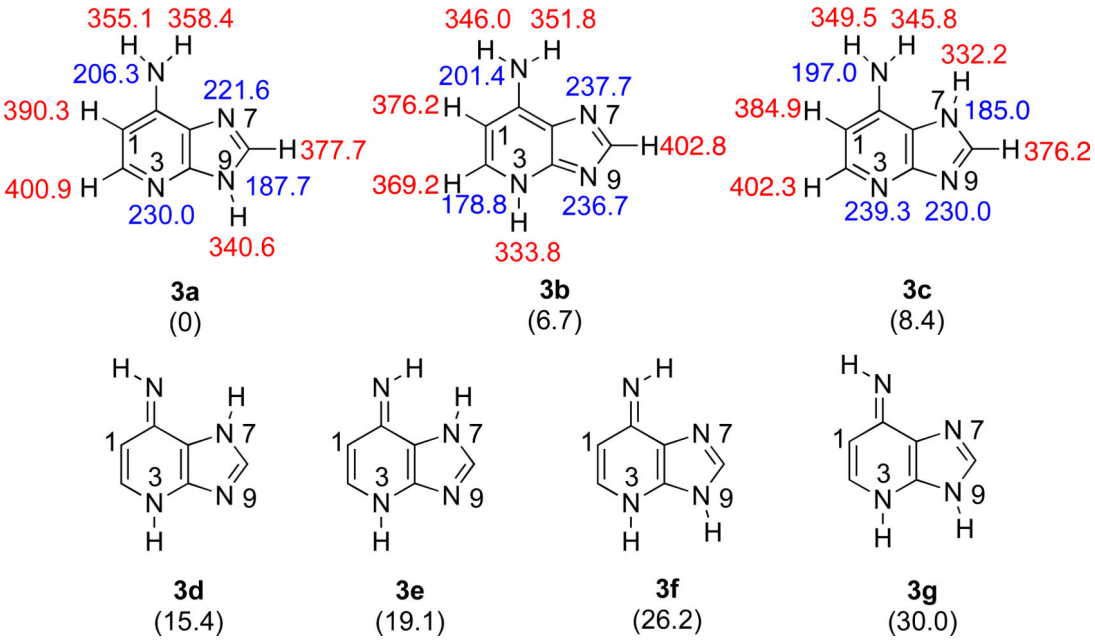

Figure 5.

The seven possible tautomeric structures of 1-deazaadenine (Z1). Gas phase acidities are in red; gas phase proton affinities are in blue. Relative stabilities are in parentheses. Calculations were conducted at B3LYP/6-31+G(d); reported values are ΔH at 298 K.

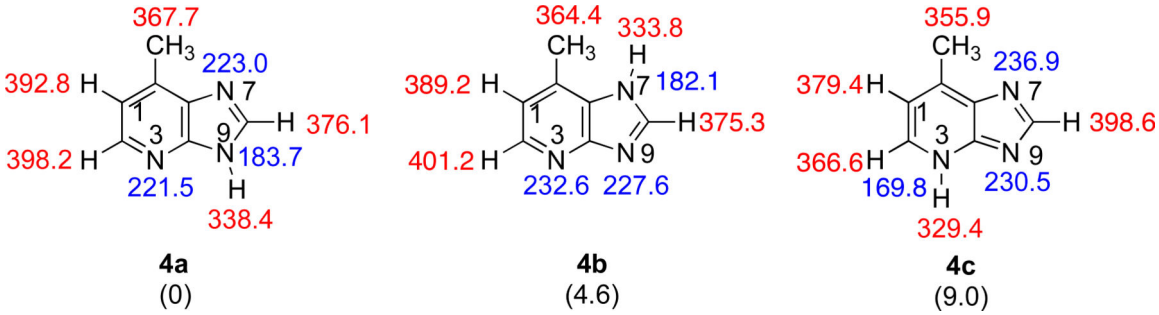

Figure 6.

The three possible tautomeric structures of Q. Gas phase acidities are in red; gas phase proton affinities are in blue. Relative stabilities are in parentheses. Calculations were conducted at B3LYP/6-31+G(d); reported values are ΔH at 298 K.

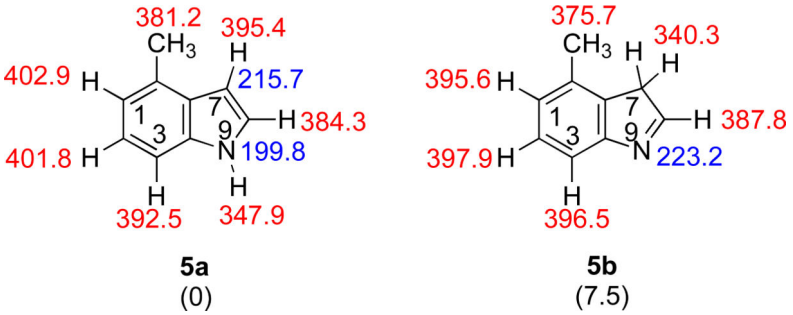

Figure 7.

The two possible tautomeric structures of M. Gas phase acidities are in red; gas phase proton affinities are in blue. Relative stabilities are in parentheses. Calculations were conducted at B3LYP/6-31+G(d); reported values are ΔH at 298 K.

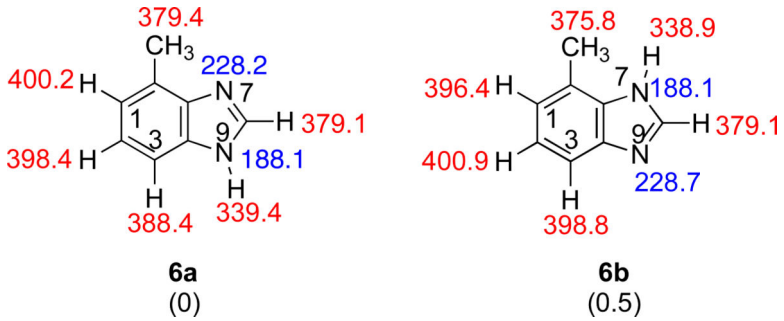

Figure 8.

The two possible tautomeric structures of B. Gas phase acidities are in red; gas phase proton affinities are in blue. Relative stabilities are in parentheses. Calculations were conducted at B3LYP/6-31+G(d); reported values are ΔH at 298 K.

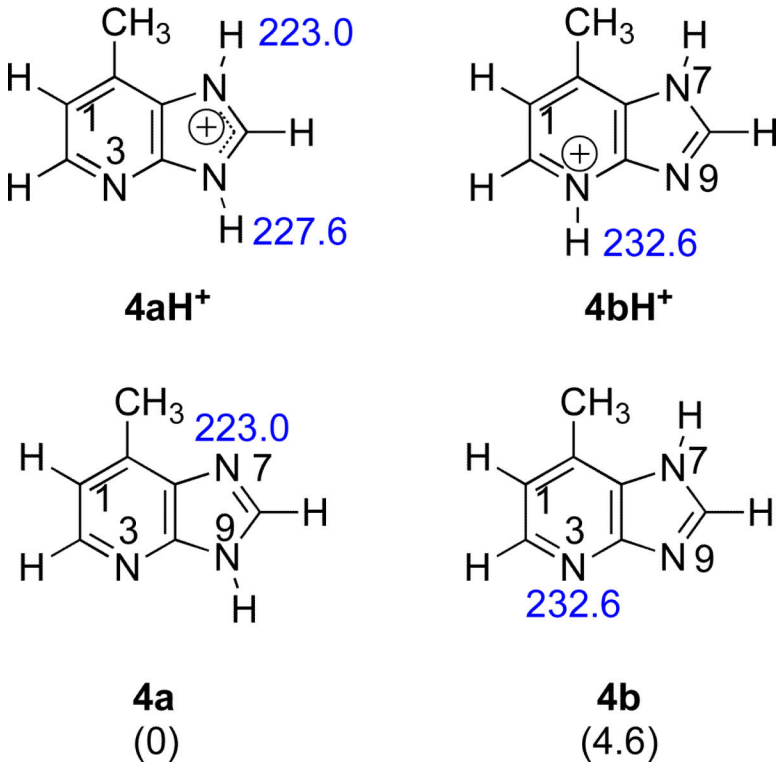

Figure 9.

Structures of **4a, 4b, 4aH**$^{+}$ and **4bH**$^{+}$ and calculated proton affinities. Relative stabilities of the two neutral tautomers are shown in parentheses. Calculations were conducted at B3LYP/6-31+G(d) [ΔH at 298 K in kcal mol^{-1}].

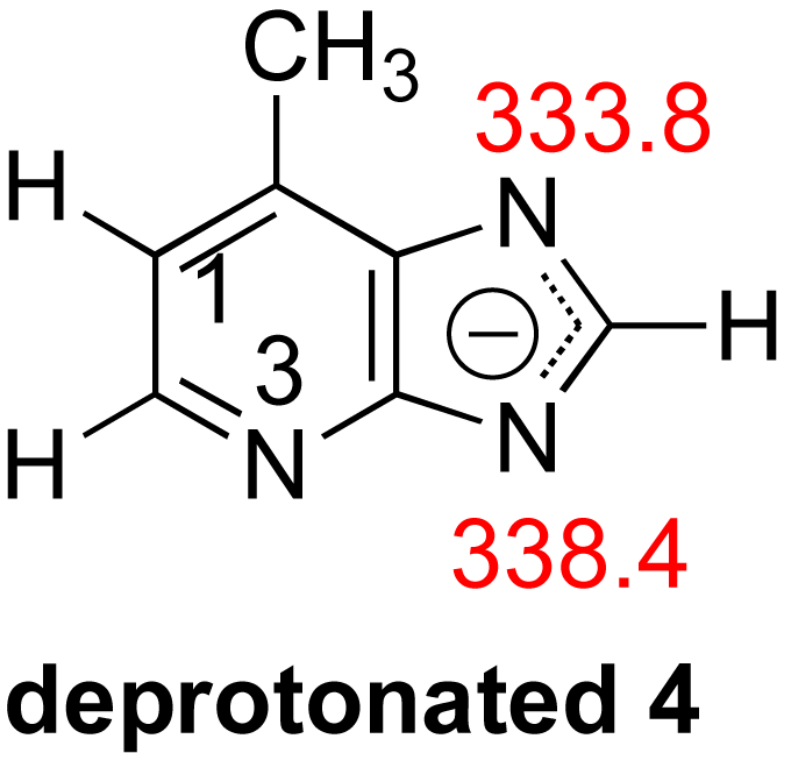

Figure 10.
Structure of deprotonated **4a** and **4b** and calculated acidities. Calculations were conducted at B3LYP/6-31+G(d) [ΔH at 298 K in kcal mol^{-1}].

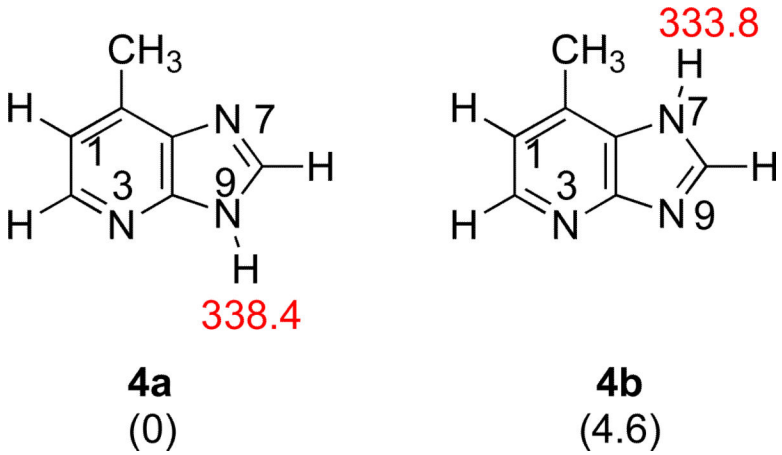

Figure 11.

Structures of **4a** and **4b** and calculated acidity of the most acidic site. Relative stabilities of the two neutral tautomers are shown in parentheses. Calculations were conducted at B3LYP/6-31+G(d) [ΔH at 298 K in kcal mol^{-1}].

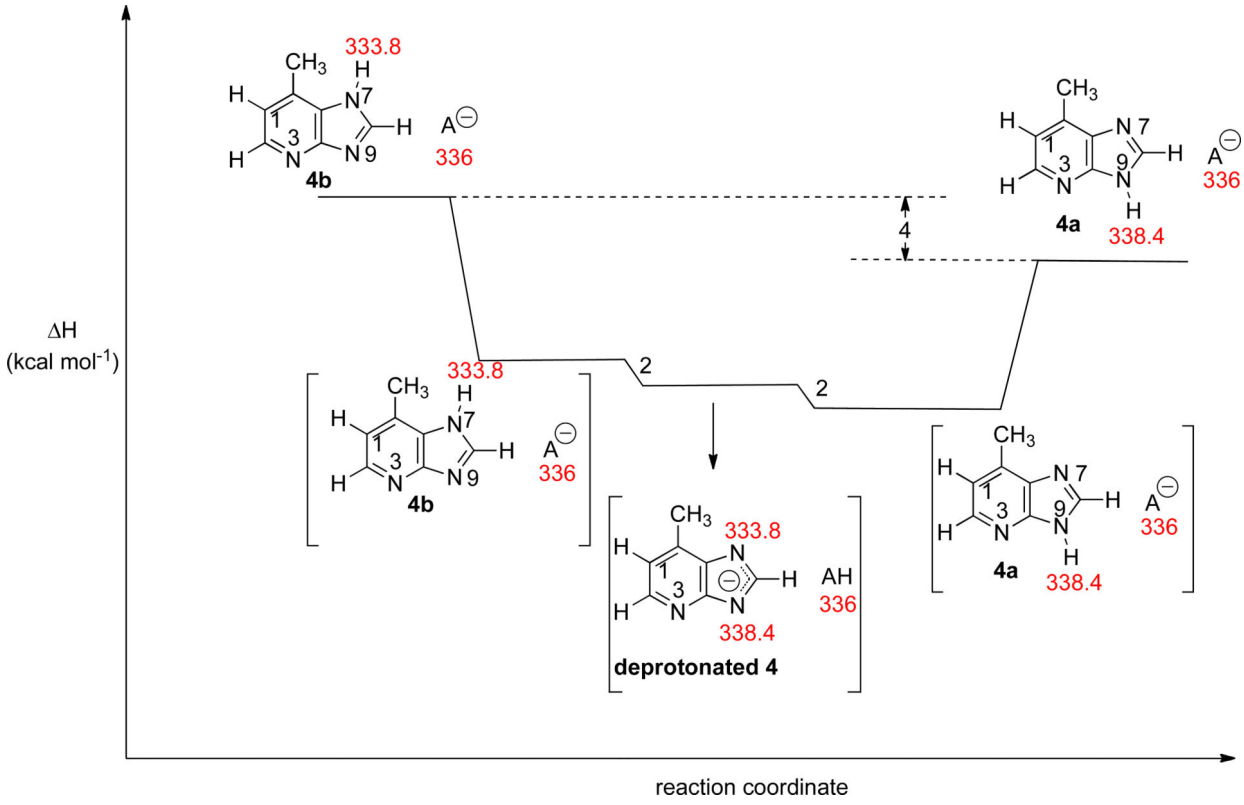

Figure 12.

Reaction coordinate for the base-catalyzed tautomerization of **4b** to **4a**. "A^-" represents deprotonated reference acid. Values in red are B3LYP/6-31+G(d) calculated ΔH_{acid} values (298 K).

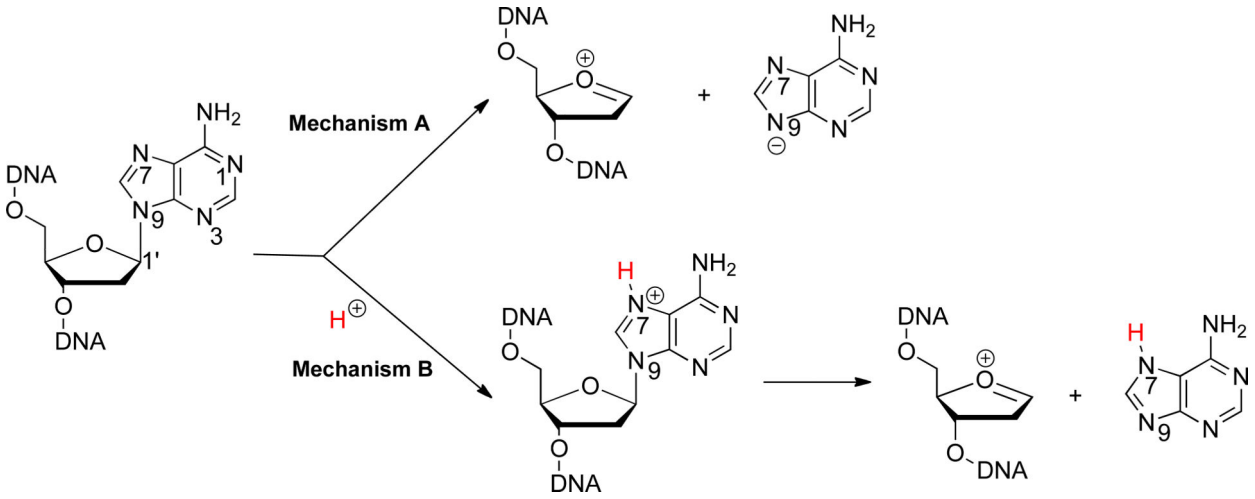

Scheme 1.

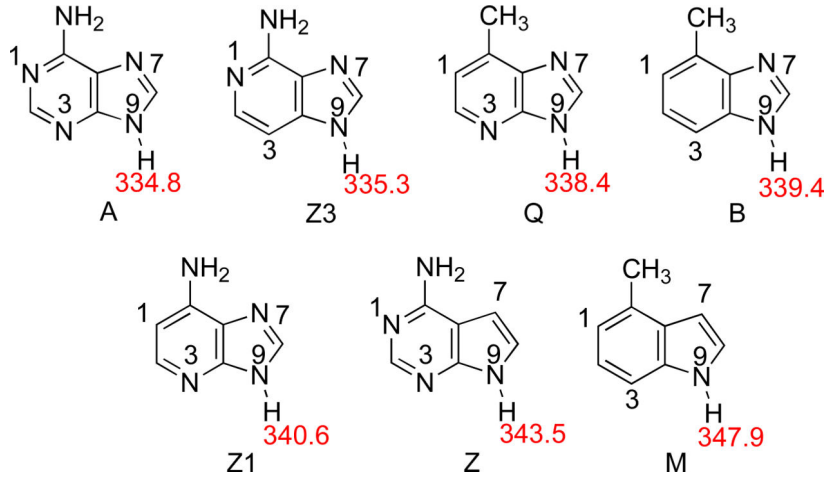

Figure 13.

Calculated (B3LYP/6-31+G(d)) gas phase acidities (ΔH, kcal mol^{-1}) of the N9-H for neutral adenine analogs. Substrates are ordered in decreasing acidity (increasing ΔH_{acid} value).

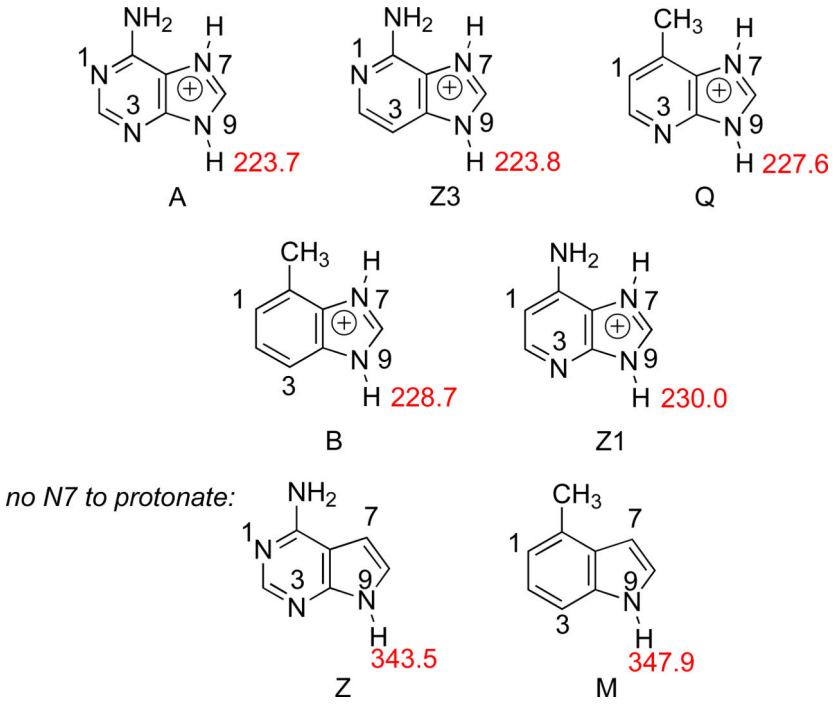

Figure 14.

Calculated (B3LYP/6-31+G(d)) gas phase acidities (kcal mol^{-1}) of the N9-H for N7-protonated nucleobase analogs. (Z and M have no N7 to protonate; acidities are shown for comparison). Substrates are ordered in decreasing acidity (increasing ΔH_{acid} values).

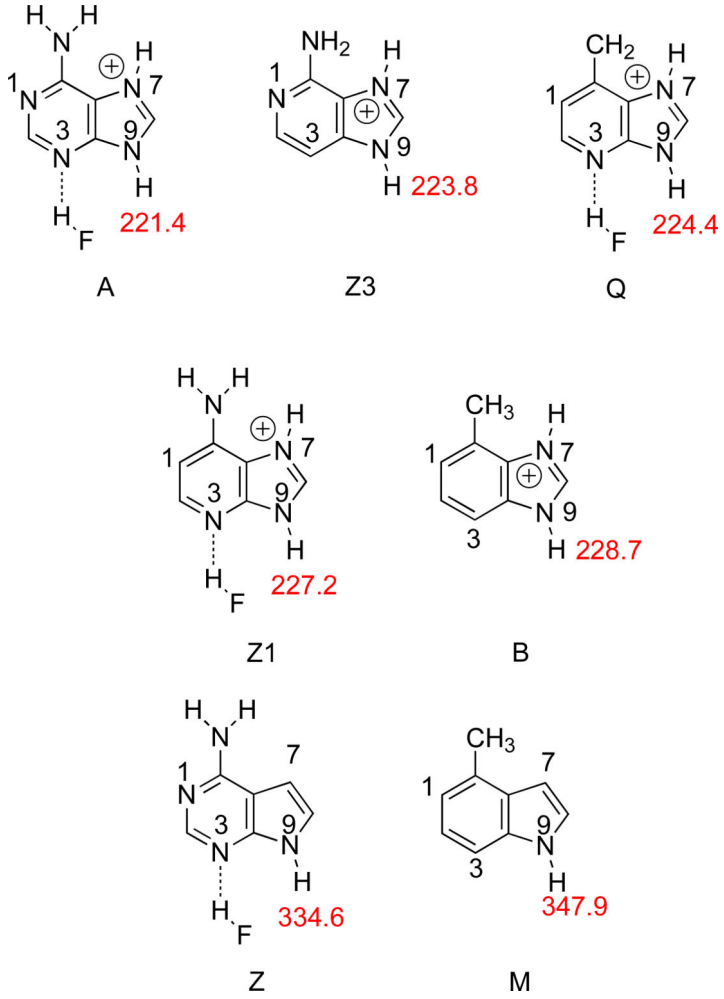

Figure 15.

Calculated (B3LYP/6-31+G(d)) gas phase acidities (kcal mol^{-1}) of the N9-H for N7-protonated, N3-hydrogen-bonded adenine analogs. Substrates are ordered in decreasing acidity (increasing ΔH_{acid} values).

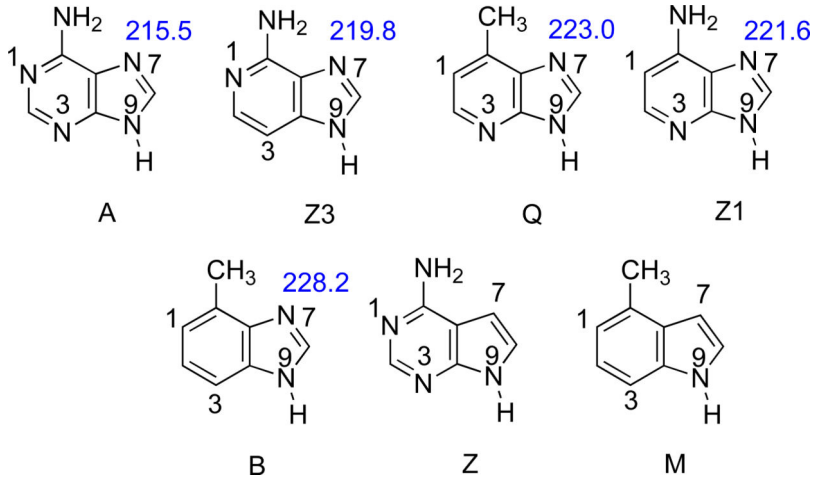

Figure 16.

Calculated (B3LYP/6-31+G(d)) gas phase PAs (ΔH, kcal mol^{-1}) of the N7 for adenine and analogs. Substrates are ordered in increasing PA.

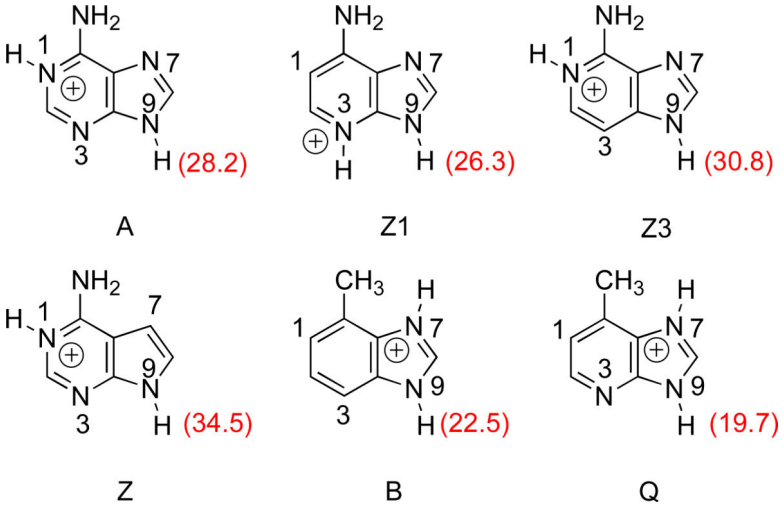

Figure 17.

Aqueous N9-H acidities (kcal mol^{-1}) of nucleobase analogs with the most basic site protonated.

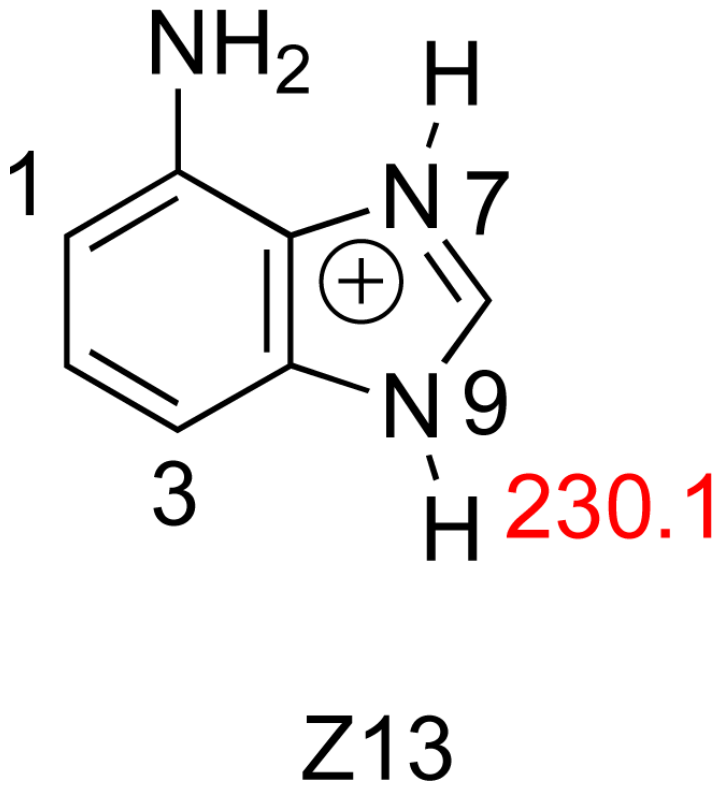

Figure 18.
Calculated (B3LYP/6-31+G(d)) gas phase acidities (ΔH, kcal mol^{-1}) of the N9-H for N7-protonated nucleobase analog Z13.

Table 1

Summary of results for acidity bracketing of Z (7-deazaadenine, 1).

Reference compound	ΔH_{acid} [a]	Proton transfer[b]	
		Ref. acid	Conj. base
m-cresol	349.5 ± 2.1	–	+
acetic acid	347.4 ± 0.5	–	+
butyric acid	346.8 ± 2.0	+	+
formic acid	346.0 ± 0.5	+	–
methacrylic acid	344.1 ± 2.9	+	–
methyl cyanoacetate	340.80 ± 0.60	+	–

[a] Acidities are in kcal mol^{-1}.[31,32]

[b] A "+" indicates the occurrence and a "–" indicates the absence of proton transfer.

Table 2

Summary of results for proton affinity bracketing of Z (7-deazaadenine, 1)

Reference compound	PA[a]	Proton transfer[b]	
		Ref. base	Conj. acid
1-methylpiperidine	232.1 ± 2.0	+	–
1-methylpyrrolidine	230.8 ± 2.0	+	–
piperidine	228.0 ± 2.0	+	+
pyrrolidine	226.6 ± 2.0	–	+
3-picoline	225.5 ± 2.0	–	+

[a] PAs are in kcal mol^{-1}.[31]

[b] A "+" indicates the occurrence and a "–" indicates the absence of proton transfer

Table 3

Summary of results for acidity bracketing of Z3 (3-deazaadenine, 2)

Reference compound	ΔH_{acid} [a]	Proton transfer [b]	
		Ref. acid	Conj. base
methyl cyanoacetate	340.80 ± 0.60	–	+
trifluoro-*m*-cresol	339.3 ± 2.1	–	+
2-chloropropanoic acid	337.0 ± 2.1	+	+
malononitrile	335.8 ± 2.1	+	–
pyruvic acid	333.5 ± 2.9	+	–
difluoroacetic acid	331.0 ± 2.2	+	–

[a] Acidities are in kcal mol^{-1}.31

[b] A "+" indicates the occurrence and a "–" indicates the absence of proton transfer.

Table 4

Summary of results for proton affinity bracketing of Z3 (3-deazaadenine, 2)

Reference compound	PA[a]	Proton transfer[b]	
		Ref. base	Conj. acid
2,2,6,6-tetramethylpiperidine	235.9 ± 2.0	+	–
N,*N*-dimethylcyclohexylamine	235.1 ± 2.0	+	–
triethylamine	234.7 ± 2.0	+	–
di-sec-butylamine	234.4 ± 2.0	+	–
1-methylpiperidine	232.1 ± 2.0	–	+
N,*N*-dimethylisopropylamine	232.0 ± 2.0	–	+
1-methylpyrrolidine	230.8 ± 2.0	–	+
piperidine	228.0 ± 2.0	–	+

[a] PAs are in kcal mol^{-1}.31

[b] A "+" indicates the occurrence and a "–" indicates the absence of proton transfer

Table 5

Summary of results for acidity bracketing of Q (4).

Reference compound	ΔH_{acid} [a]	Proton transfer [b]	
		Ref. acid	Conj. base
formic acid	346.0 ± 0.5	–	+
methacrylic acid	344.1 ± 2.9	–	+
2,4-pentanedione	343.8 ± 2.1	–	+
methyl cyanoacetate	340.80 ± 0.60	+	+
trifluoro-*m*-cresol	339.2 ± 2.1	+	–
2-chloropropanoic acid	337.0 ± 2.1	+	–

[a] Acidities are in kcal mol^{-1}.[31,32]

[b] A "+" indicates the occurrence and a "–" indicates the absence of proton transfer.

Table 6

Summary of results for proton affinity bracketing of Q (4).

Reference compound	PA[a]	Proton transfer[b]	
		Ref. base	Conj. acid
1-methylpiperidine	232.1 ± 2.0	+	–
1-methylpyrrolidine	230.8 ± 2.0	+	–
piperidine	228.0 ± 2.0	+	+
pyrrolidine	226.6 ± 2.0	+	+
4-picoline	226.4 ± 2.0	+	+
3-picoline	225.5 ± 2.0	+	+
pyridine	223.8 ± 2.0	–	+
n-octylamine	222.0 ± 2.0	–	+

[a] PAs are in kcal mol^{-1}.[31]

[b] A "+" indicates the occurrence and a "–" indicates the absence of proton transfer

Table 7

Summary of results for acidity bracketing of B (6).

Reference compound	ΔH_{acid} [a]	Proton transfer[b]	
		Ref. acid	Conj. base
methacrylic acid	344.1 ± 2.9	–	+
2,4-pentanedione	343.8 ± 2.1	–	+
methyl cyanoacetate	340.80 ± 0.60	+	–
trifluoro-*m*-cresol	339.2 ± 2.1	+	–
malononitrile	335.8 ± 2.1	+	–

[a] Acidities are in kcal mol^{-1}.[31,32]

[b] A "+" indicates the occurrence and a "–" indicates the absence of proton transfer.

Table 8

Summary of results for proton affinity bracketing of B (6).

Reference compound	PA[a]	Proton transfer[b]	
		Ref. base	Conj. acid
1-methylpiperidine	232.1 ± 2.0	+	–
1-methylpyrrolidine	230.8 ± 2.0	+	–
piperidine	228.0 ± 2.0	+	+
pyrrolidine	226.6 ± 2.0	–	+
3-picoline	225.5 ± 2.0	–	+

[a] PAs are in kcal mol^{-1}.[31]

[b] A "+" indicates the occurrence and a "–" indicates the absence of proton transfer

Table 9

MutY excision of nucleobase analogs opposite OG within 30 bp DNA substrates.

Nucleobase analog	k_g (min^{-1})[a]	Fold reduced relative to OG:A substrate
A	12 ± 2[c]	---
Q (**4**)	1.2 ± 0.2[c]	10x
Z1 (**3**)	0.31 ± 0.06	40x
Z3 (**2**)	0.10 ± 0.05[b]	100x
B (**6**)	< 0.002[c]	6000x
M (**5**)	NC[d,e]	>24,000x
Z (**1**)	NC[e]	>24,000x

fValue previously reported (reference[28]).

[a]Rates were measured at 37° C. Errors represent standard deviation from the average.

[b]Value previously reported (reference[26]).

[c]Value previously reported (reference[25]).

[d]Not cleaved above detection limit (<0.0005 min^{-1}).

[e]Value previously reported (reference[27]).

Table 10

Relative cleavage of nucleobase analogs in acidic aqueous solution.

Nucleobase	Extent of acid-catalyzed depurination (normalized to A)
A	1
Z3	0.3[a]
Z1	7[a]
B	2[b]
Q	7[b]

[a] This work.

[b] Reference 25

Table 11

Calculated (B3LYP/6-31+G(d); 298 K) and experimental data

Substrate	Calculated value	Experimental value[b]
ΔH_{acid}[a]		
Z (**1**)	343.5	347
Z3 (**2**)	335.3	337
Z1 (**3**)	340.6	(341)
Q (**4**)	338.4	341
M (**5**)	347.9	(349)
B (**6**)	339.4	343
adenine	334.8[c]	333 (335)[c]
PA[a]		
Z (**1**)	228.4	228
Z3 (**2**)	233.2	233
Z1 (**3**)	230.0	(232)
Q (**4**)	223.0	223.8-230.8
M (**5**)	215.7	N/A
B (**6**)	228.2	228
adenine	223.7[c]	224 (225)[c]

[a] ΔH_{acid} and PA values are in kcal mol^{-1}

[b] Nonparenthetical experimental value is from bracketing measurement; Cooks kinetic method value is in parentheses. Error is ±3-4 kcal mol^{-1}.

[c] References 21,22,34

Table 12

HYPOTHETICAL bracketing table if only 4a were present.

Reference compound	PA[a]	Proton transfer[b]	
		Ref. base	Conj. acid
1-methylpiperidine	232.1 ± 2.0	+	–
1-methylpyrrolidine	230.8 ± 2.0	+	–
piperidine	228.0 ± 2.0	+	–
pyrrolidine	226.6 ± 2.0	+	–
4-picoline	226.4 ± 2.0	+	–
3-picoline	225.5 ± 2.0	+	–
pyridine	223.8 ± 2.0	–	+
n-octylamine	222.0 ± 2.0	–	+